Scientia Iranica, Vol. 15, No. 3, pp 332–339

SCIENTIA
IRANICA

Investigation of the Effect of Pad Geometry on Flat and Rounded Fretting Fatigue

A. Mohajerani[1] and G.H. Farrahi[*]

In this paper, the effect of geometrical parameters on the fretting fatigue of a half-plane in contact with a flat and rounded pad is studied. This is accomplished by calculating and comparing the stress states and stress intensity factors of fretting cracks for a number of pad geometries. The pad geometry is represented by the radius of its rounded corners and the width of its central flat part. The distribution of dislocation method is employed to calculate the stress intensity factors of fretting induced cracks of different lengths for different values of geometrical parameters. The results of this study can be insightful for improving the geometrical design of an aero-engine compressor disk, as similar contact and damage are prone to occur in its dovetail region.

INTRODUCTION

Fretting fatigue is damage caused by a reduction of fatigue strength, due to low-amplitude oscillatory sliding motions occurring between contacting surfaces. This damage is responsible for much premature failure of disks and blades in turbine engines and, therefore, has been the focus of many studies [1-10]. The assemblage of these components is normally undertaken by using dovetail or fir-tree shaped attachments. The dovetail region of aeroengine compressor disks experiences fretting in a flat-on-flat contact with a relatively large radius at the edge of the contact [11]. Some studies have been conducted to directly investigate cracks and stress states in the dovetail region [1,12-14]. Since experimental setups are costly and stress states are mostly unknown, simplified models of the dovetail region are widely used for analysis purposes. One such model is that of a flat and rounded pad in contact with a half-plane placed under the fretting loading. This model is favorable because of its similarity to the mechanism of contact in the dovetail region and also its analytical tractability [11,15-20].

In the present work, the effect of pad geometry on the fretting fatigue of a half-plane, in the aforementioned model, is studied. This is accomplished by calculating and comparing stress states and Stress Intensity Factors (SIF) of fretting cracks for a number of pad geometries. The geometry of the pad is represented by the radius of its rounded corners and the width of its central flat part. Knowledge of the effect of these geometrical parameters on the stress states and the SIFs of the fretting cracks will help improve the dovetail attachment geometry designs.

To calculate the SIFs of fretting fatigue cracks, the distribution of dislocations method is used, which is based on the numerical solution of integral equations [21]. First, the stress states in the half-plane are calculated for each of the pad geometries. Next, cracks with a variety of lengths at the contact boundary are considered and their SIFs are calculated in respect to each of the pad geometries. A sample model is analyzed using the Finite Element Method (FEM) to verify the results.

STRESS STATE IN THE HALF-PLANE

Normal and Shear Traction Calculation

In this section, the method used to calculate stress states are described, in respect to a typical geometry of the pad. Figure 1 shows the configuration of the contact model. The contact area has a width of $2a$ and the stick zone width is $2c$. The pad has a flat central part of width $2b$ and two rounded corners of radius R. These corners are approximated by parabolic curves. As shown, the half-plane is subjected to, not only the normal force, P, and the tangential force, Q, but also a bulk stress, σ_b. Due to the exertion of bulk stress to the half-plane, the stick zone shifts by the value of e and

1. *Department of Mechanical Engineering, Sharif University of Technology, Tehran, I.R. Iran.*
*. *Corresponding Author, Department of Mechanical Engineering, Sharif University of Technology, Tehran, I.R. Iran. E-mail: farrahi@sharif.edu*

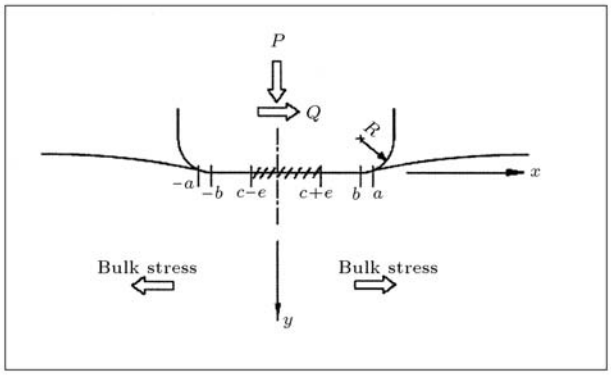

Figure 1. A schematics illustration of a flat and rounded contact configuration.

the shear traction distribution becomes asymmetric. Although the presence of bulk stress results in more complications in analytical solutions, it should be taken into account, as the fretting fatigue normally takes place in the presence of bulk stresses within one or both of the contacting bodies, due to loadings other than the contact itself.

When the flat rounded pad and half-plane have the same modulus of elasticity, E, and Poisson ratio, v, the equation used to calculate the normal traction, $p(x)$, can be written as [16]:

$$\pi ARp(x) = x \ln \frac{\left(b\sqrt{a^2-x^2} + x\sqrt{a^2-b^2}\right)^2}{a^2\left|x^2-b^2\right|} - b \ln \frac{\left(\sqrt{a^2-b^2} + \sqrt{a^2-x^2}\right)^2}{\left|x^2-b^2\right|} + 2\sqrt{a^2-x^2} \arccos\frac{b}{a}, \quad (1)$$

where A is given by:

$$A = \frac{\kappa+1}{2G},$$

$$\kappa = \begin{cases} 3-4v & \text{for plane strain} \\ \frac{3-v}{1+v} & \text{for plane stress} \end{cases} \quad (2)$$

As G is the modulus of rigidity. In this paper, only cases of moderate bulk stresses are considered, for which tangential traction has the same sign over the entire contact area. Using the relation between shear traction, $q(x)$, and the tangential relative slip of surface points, $g(x)$, the unknown $q(x)$ is calculated:

$$\frac{1}{A}\frac{\partial g}{\partial x} = \frac{1}{\pi}\int_{-a}^{a} \frac{q(\zeta)}{\zeta - x} d\zeta - \frac{\sigma_b}{4}. \quad (3)$$

The shear traction can be defined as:

$$q(x) = q^*(x) + f|p(x)|, \qquad |x-e| \le c,$$

$$q(x) = f|p(x)|, \qquad a \le x \le -c+e \cup c+e \le x \le a, \quad (4)$$

where f is the coefficient of friction. In the stick zone, there should be no relative movement ($\partial g/\partial x = 0$). Thus, by substituting Equation 4 into Equation 3 in the stick zone, one obtains:

$$\frac{\sigma_b}{4} - \frac{1}{\pi}\int_{-a}^{a} \frac{f|p(x)|}{\xi - x} d\xi = \int_{e-c}^{e+c} \frac{q^*(\xi)}{\xi - x} d\xi. \quad (5)$$

The Gauss-Chebyshev quadrature method can be used to solve Equation 5 [22]. The same procedure that is used in [23] is applied here to find the shear traction at certain points. The stick zone shift and σ_b are related variables and only one of them can be chosen arbitrarily. The relation between these variables can be found by invoking the consistency condition [24]. Through the calculation of normal and shear tractions on the contact surface, the values of normal and tangential forces can be found using the equilibrium conditions of the pad [16].

Interior Stress State

The stress state in the half-plane is given by the superposition of the contact-induced stress state and the bulk stress. In order to evaluate the contact-induced stress state, the pressure and the shear tractions are considered as arrays of overlapping triangular traction elements. The use of such elements results in a piecewise linear approximation to the surface tractions and is, thus, free from discontinuities associated with the piecewise method [25]. The stress state due to each traction element is calculated and used to obtain the total contact-induced stress state. For convenience, only the first component of the stress state, σ_x, is used for demonstration purposes in the following sections. However, it should be noted that this method can be applied efficiently to calculate all components of the stress.

FINITE ELEMENT MODELING

The configuration of the finite element model is shown is Figure 2. This model has been extensively used in [11,23-27] because of its similarity to most fretting fatigue experimental setups. In the finite element modeling of this configuration, the lower plate was taken as large enough to appropriately approximate a half-plane.

The model was loaded in two steps. In the first load step, normal force was applied to the pad and, in the second step, the bulk stress, σ_b, was applied to the lower plate. Note that the bulk stress automatically brings about the tangential force, Q. As shown in Figure 3, in order to create the moment, M,

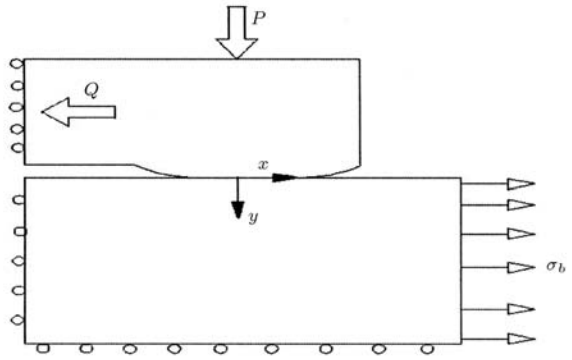

Figure 2. The configuration of the finite element model under fretting loading. Note that in order to introduce the tangential force, Q, the pad is constrained in x direction.

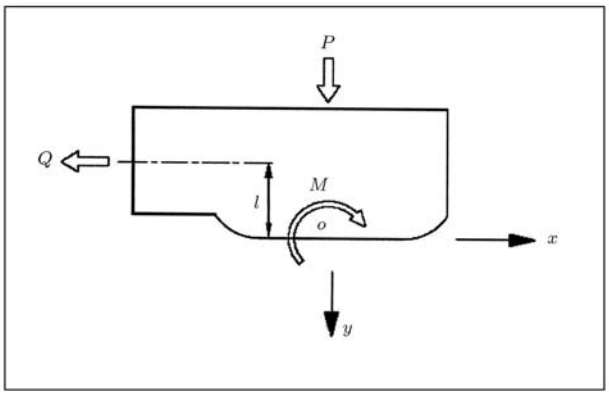

Figure 3. A schematic view of the pad loading. Static equilibrium requires the pressure distribution to be asymmetrical to make the moment (M), opposite to the moment created by the tangential force around the contact center (o).

necessary for the equilibrium of the pad, the pressure distribution over the contact surface should be asymmetric. However, pressure distribution in homogeneous contacts should be independent of tangential loads. The symmetry of pressure distribution is a significant concern in the finite element modeling, and can be significantly overcome by coupling the nodes of the pad's upper side in the y direction. The size and number of the crack tip singular elements were chosen according to [26].

The model was meshed using 8-node plane elements. Mesh refinement was undertaken in multiple steps. At each step, the model was run and the stress values at some points of interest were recorded. The mesh refinement was quitted when these stress values were stabilized.

In contrast to the contact mechanics approach of analyzing the stress state, in which the Q value is an input to the problem, in this finite element model, Q could not be prescribed directly into the model. The value of Q is affected by many factors, such as the length and elasticity modulus of the pad arm (i.e. the extended side of the pad in Figure 2) and the bulk stress. In the current model, the pad arm was defined by a new set of material properties, so that its E values could be adjusted for obtaining the desired Q value. The adopted trial and error approach required several runs of the model for the number of E values of the pad arm and for recording the corresponding Q values. Finally, an E value for the pad arm was found that corresponds to an acceptable value of Q.

DISTRIBUTION OF DISLOCATIONS METHOD

The distribution of dislocations method is a convenient approach for calculating the SIFs of cracks in half-planes under complicated stress states [21,27]. This method is based on the numerical solution of integral equations that relates the relative displacement of the crack faces to the stress state of an uncracked half-plane. Once the relative displacements of the crack faces are calculated, the SIFs can be obtained using the well-known fracture mechanics relations of the SIFs and the relative displacement of the crack faces. In this method, first the stress values along the line of the crack are obtained in its absence. Then, a distribution of dislocations is introduced along the line of the crack. Let $N(x)$ be introduced as the total normal traction across the crack, and $\sigma_T(x)$ as the stress along the line of the crack in its absence. Based on the coordinate system depicted in Figure 4, the mentioned integral equation for cracks of length b can be written as [21]:

$$N(x) = \sigma_T(x) + \frac{G}{\pi(\kappa+1)} \int_0^b B_y(c) K(x,c) dc. \qquad (6)$$

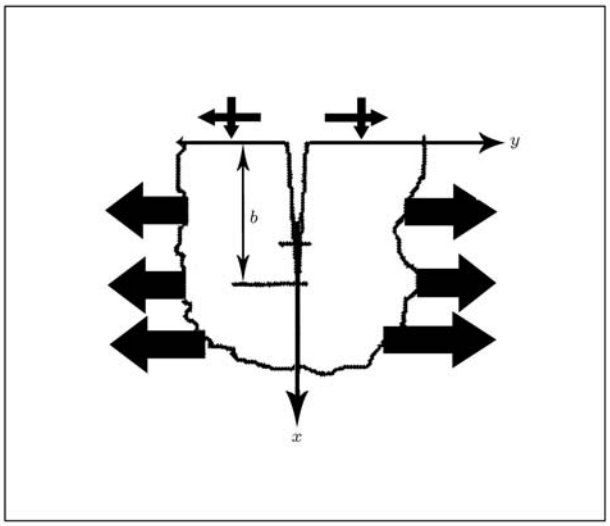

Figure 4. A normal crack in a half-plane with the length b.

It should be noted that for traction free crack faces, $N(x)$ is zero. In the above equation, $B_y(c)$ is the density of the distribution of dislocations given by:

$$B_y(c) = \frac{db_y}{dx}(c), \tag{7}$$

where b_y is the length of the dislocation burger vector, which in the case of the present work is directed in the y direction. $K(x,c)$ is a generalized Cauchy kernel given by:

$$K(x,c) = 2\left\{\frac{1}{x-c} - \frac{1}{x+c} - \frac{2c}{(x+c)^2} + \frac{4c^2}{(x+c)^3}\right\}. \tag{8}$$

The first step involved in the numerical solution of Equation 6 is to normalize the variables by introducing new variables given by:

$$s = \frac{2x}{b} - 1, \qquad r = \frac{2c}{b} - 1. \tag{9}$$

And by switching to a series representation, such that a system of simultaneous linear algebraic equations remains, the following is obtained:

$$\frac{b}{2}\times\frac{G}{\pi(k+1)}\sum_{i=1}^{n}\frac{2\pi(1+r_i)}{2n+1}K(s_k,r_i)\phi(r_i) = -\sigma_T(s_k).$$

By calculating the values of $\phi(r_i)$, $\phi(1)$ can be obtained as follows:

$$\phi(1) = \frac{2}{2n+1}\sum_{i=1}^{n}\cot\left(\frac{\zeta}{2}\right)\sin(n\zeta)\,\phi(r_i), \tag{10}$$

where $\zeta = \frac{(2i-1)\pi}{2n+1}$. Finally, the first mode stress intensity factor, denoted by K_I, can be obtained:

$$K_I = 2\sqrt{2}\sqrt{\pi b}\frac{G}{(\kappa+1)}\phi(1). \tag{11}$$

A similar approach can be applied to obtain the mode II stress intensity factor, K_{II}.

DISCUSSION AND RESULTS

The role of pad geometry on fretting fatigue is studied by observing the effect of varying each geometrical parameter on the half-plane stress states and SIFs of fretting.

Three values are considered for the radius of the pad corners, R, as 50, 100 and 140 mm. For each R value, the width of the central flat part of the pad, $2b$, is taken as 3, 6, 10 or 16 mm.

Consideration of the mentioned values for b and R results to twelve pad geometries. For each of these 12 pad geometries, the SIFs were calculated for a number of cracks with lengths from 0.1 mm to 1 mm. The plane strain state was assumed. The other specifications of the models are shown in Table 1.

Table 1. The specifications of the contact model used in the study.

E (MPa)	v	f	P (N)	Q (N)	σ_b (MPa)
126000	0.3	0.5	896	376	23.7

Since the values of a, c and e vary in accordance with R and b, their values should first be calculated, using the contact equilibrium equations and consistency conditions for each of the contact geometries [16,23].

The effect of pad geometry on stress states in the half-plane are studied for each of the four cases shown in Table 2, where the highest and lowest values for R and b have been chosen in their mentioned intervals to accentuate the effect of parameter variations. Using the method described previously, the value of the x-component of the normal stress, σ_x, at the depth of 0.1 mm (y = 0.1 mm), was calculated for each case. Figure 5 depicts the value of σ_x for the four cases. A peak value of σ_x can be observed near the contact boundary. It can be seen that increasing b and R reduces the peak value of σ_x. Also, note that, as the flat part width of the pad increases, the effect of corner radius on the peak value of σ_x is weakened.

Table 2. The geometrical parameters of the pads for the cases shown in Figure 5. In each case, the highest or lowest value of each parameter is chosen for a better comparison of the resulting stress states.

Case No.	1	2	3	4
b	8	8	1.5	1.5
R	50	140	140	50

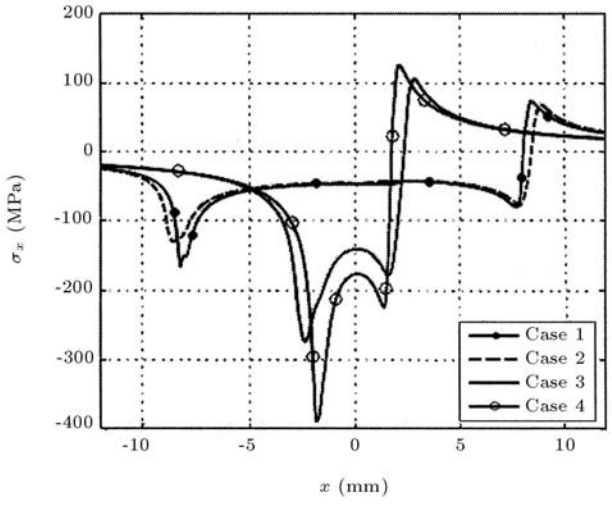

Figure 5. The values of σ_x in respect to four pad geometries, in the depth of 0.1 mm.

A sample case was studied by FEM to verify the results. For this sample model, parameters are chosen to be $b = 5$ and $R = 100$. As shown in Figure 6, the values of σ_x, at the depth of 0.1 mm, are in good agreement with FEM results. The values of K_I for cracks with different lengths in this model, are shown in Figure 7.

In order to investigate the effect of pad geometry on the SIF of fretting cracks, the first mode stress intensity factor, K_I, versus crack length, is illustrated in Figures 8, 9 and 10 for $R = 50$, 100 and 140 mm, respectively.

As shown in Figures 8, 9 and 10, the effect of pad flat part width, b, on the value of K_I, is highly affected by crack length. For shorter cracks, increasing b results in the decrease of K_I. However, for cracks longer than a critical value, the effect of b on K_I is

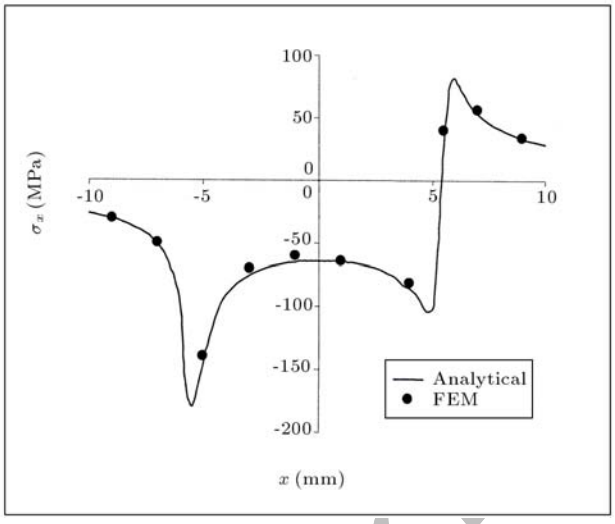

Figure 6. σ_x in the depth of 0.1 mm in the sample model.

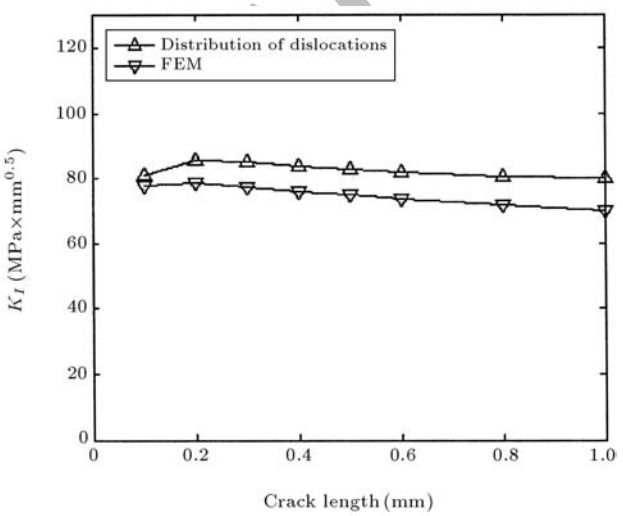

Figure 7. The K_I values vs. crack length in the sample model.

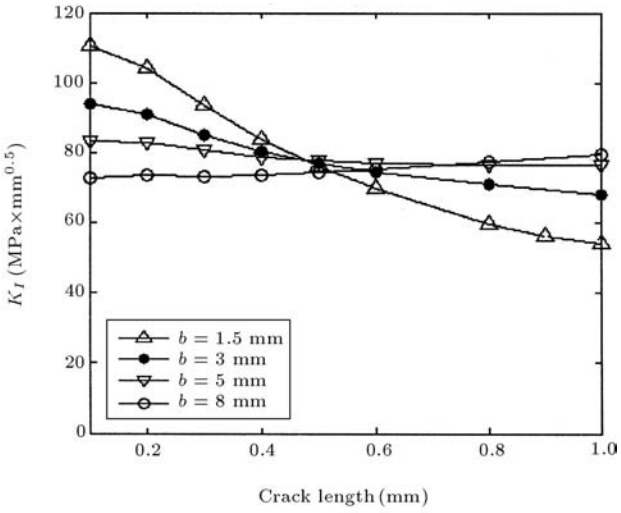

Figure 8. K_I values vs. crack length for $R = 50$ mm.

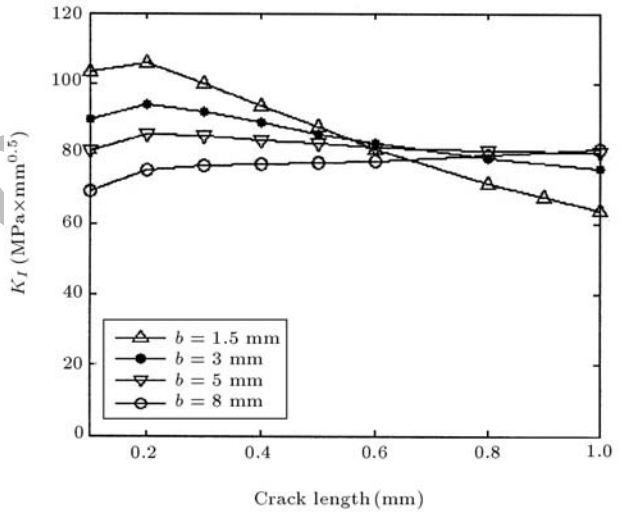

Figure 9. K_I values vs. crack length for $R = 100$ mm.

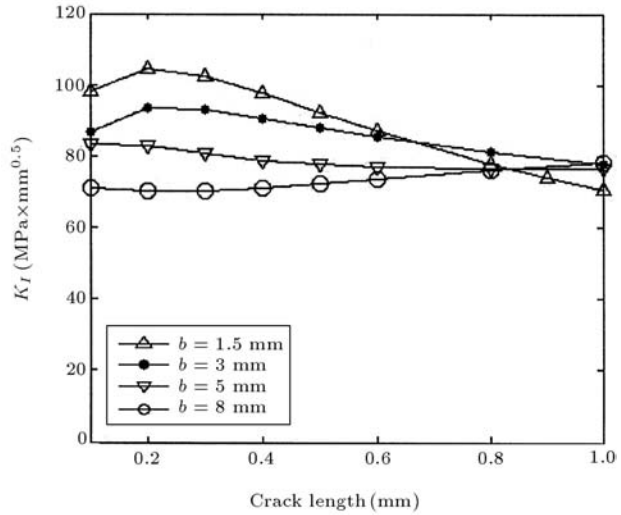

Figure 10. K_I values vs. crack length for $R = 140$ mm.

reversed. This critical crack length varies, according to the values of R.

Although K_I and its variations have been the main concern of most fatigue studies, knowledge about K_{II} values is essential too, for fretting fatigue studies. Therefore, the effect of pad geometry on K_{II} values has also been investigated using the same methods and assumptions employed for the study on the first mode of stress intensity factors.

The K_{II} values of the cracks in the sample model, calculated by FEM, and the distribution of dislocations method are shown in Figure 11. The K_{II} values of cracks with different lengths for $R = 50$, 100 and 140 mm are shown in Figures 12, 13 and 14, respectively. As shown, increasing R and b can significantly reduce the K_{II} values.

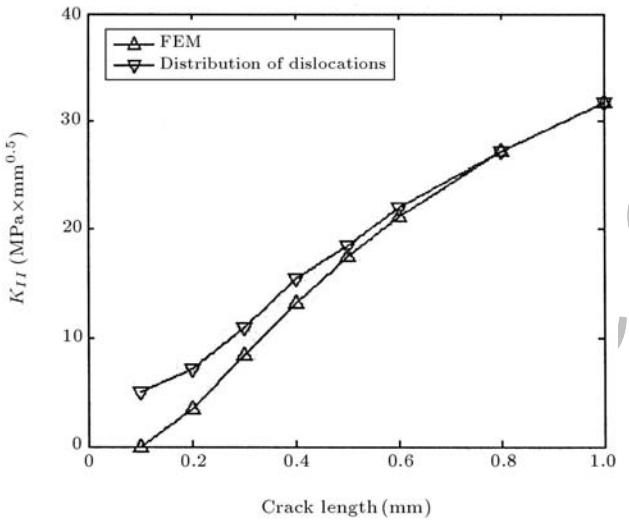

Figure 11. The K_{II} values vs. crack length in the sample model.

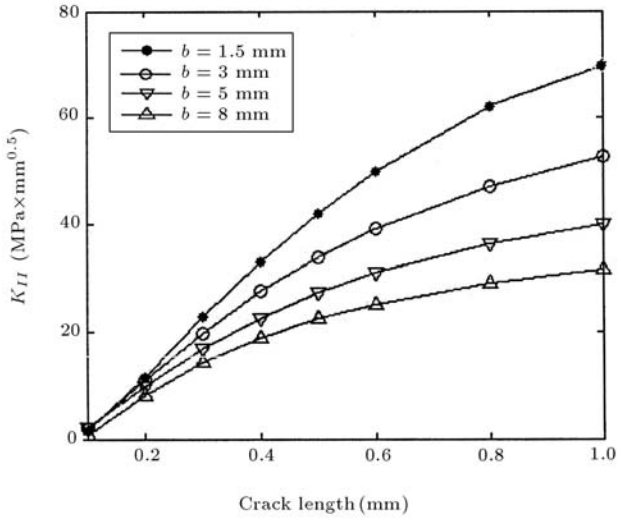

Figure 12. K_{II} values vs. crack length for $R = 50$ mm.

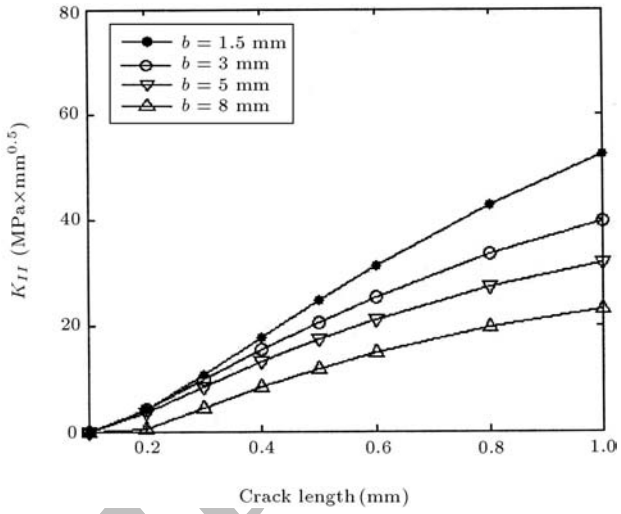

Figure 13. K_{II} values vs. crack length for $R = 100$ mm.

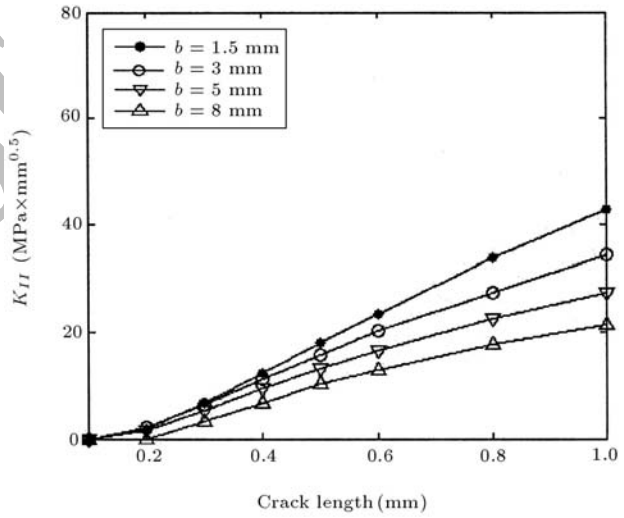

Figure 14. K_{II} values vs. crack length for $R = 140$ mm.

CONCLUSIONS

In this paper, the effect of geometrical parameters on the fretting fatigue of a half-plane in contact with a flat and rounded pad is studied. Some of the key observations made in this work can be summarized as follows:

1. For the pads with small flat parts, the first mode stress intensity factor of the fretting crack, K_I, is almost independent of the crack length. It was also observed that increasing the pad width decreases the K_I values of short cracks and increases the K_I values of longer ones. The crack length at this turning point is highly affected by the pad corner radius. Indeed, this is the only noticeable effect of the pad radius on the values of K_I.
2. In contrast to the observations made on the vari-

ations of K_I values, a relatively consistent pattern was observed on the effect of the pad geometry on the second mode stress intensity factors, K_{II}. As the crack length increases, a consistent increase in the K_{II} values takes place. Increasing each of the geometrical parameters decreases the values of K_{II}. Although this effect is less noticeable for very short cracks, it can be clearly acknowledged for the longer ones.

Results of the study show that no general rule can be established for the assignment of a pad flat part width to minimize fretting fatigue. However, increase of the pad corner radius can consistently be a good choice for weakening the fretting fatigue.

NOMENCLATURE

a	half of the contact width
b	half the width of the pad flat part
b	crack length
b_y	length of burger vector of a normal dislocation
$B(c)$	density of distribution of dislocations
c	half of the stick zone width
e	stick zone shift from the center of contact
E	modulus of elasticity
f	coefficient of friction
G	modulus of rigidity
$g(x)$	tangential relative slip of contact points
K	generalized Cauchy kernel
K_I	first mode stress intensity factor
K_{II}	second mode stress intensity factor
M	moment created by asymmetrical pressure distribution
N	total normal traction on crack path
$p(x)$	normal traction on contact area
P	normal contact force
$q(x)$	shear traction on contact surface
Q	tangential contact force
R	radius of the pad corners
v	Poisson's ratio
σ_b	bulk stress
σ_T	normal traction on crack path due to loading

REFERENCES

1. Ruiz, C., Boddington, P.H.B. and Chen, K.C. "An investigation of fatigue and fretting in a dovetail joint", *Exp. Mech.*, **24**, pp 208-217 (1984).
2. Brryggman, U. and Soderberg, S. "Contact conditions and surface degradation mechanism in low amplitude fretting", *Wear*, **125**, pp 39-52 (1988).
3. Del Puglia, A., Pratesi, F., Zonfrillo, G. et al. "Procedure and parameters involved in fretting fatigue tests", in *Fretting Fatigue*, Waterhouse, R.B. and Lindey, T.C., Eds., ESIS 18. London: Mechanical engineering publications, pp 219-38 (1994).
4. Elkholy, A.H. "Fretting fatigue in elastic contacts due to tangential micro-motion", *Tribology Int.*, **29**(4), pp 265-75 (1996).
5. Fellows, L.J., Nowell, D. and Hills, D.A. "On the initiation of fretting fatigue cracks", *Wear*, **205**, pp 120-9 (1996).
6. Fouvry, S., Kapsa, P. and Vincent, L. "Qualification of fretting damage", *Wear*, **200**, pp 186-205 (1996).
7. Vingsbo, O. and Schon, J. "Gross slip criteria in fretting", *Wear*, **162-164**, pp 347-56 (1993).
8. Adibnazari, S. and Hoeppner, D.W. "The role of normal pressure in modeling fretting fatigue", in *Fretting Fatigue*, Waterhouse, R.B. and Lindley, T.C., Eds., ESIS 18. London: Mechanical engineering publications, pp 125-33 (1994).
9. Zhou, Z.R. and Vincent, L. "Mixed fretting regime", *Wear*, **181-183**, pp 536-51 (1995).
10. Dobromirski, J. and Smith, I.O. "Metallorgraphic aspects of surface damage, surface temperature and crack initiation in fretting fatigue", *Wear*, **117**, pp 347-57 (1987).
11. Ciavarella, M. and Macina, G. "New results for the fretting-induced stress concentration on Hertzian and flat rounded contacts", *Int. J. Mechanical Sciences*, **45**, pp 449-467 (2003).
12. Papanikos, P. and Meguid, S.A. "Theoretical and experimental studies of fretting-initiated fatigue failure of aeroengine compressor discs", *Fatigue Fract. Eng. Mater. Struct.*, **17**, p 539 (1994).
13. Papanikos, P., Meguid, S.A. and Stjepanovic, Z. "Three dimensional nonlinear finite element analysis of dovetail joints in aeroengine discs", *Finite Elements in Analysis and Design*, **29**, p 273 (1998).
14. Shlyannikov, V.N., Iltchenko, B.V. and Stepanov, N.V., *Engineering Failure Analysis*, **8**, pp 461-475 (2001).
15. Ciavarella, M., Hills, D.A. and Monno, G. "The influence of rounded edges on indentation by a flat punch", *IMechE Part C, Journal of Mechanical Engineering Science*, **212**(4), pp 319-28 (1998).
16. Jaeger, J., *Contact Mechanics*, Seville, Spain, Wessex Inst. Techn., UK, pp 307-316 (2001).
17. Hutson, A.L., Nicholas, T. and Goodman, R. "Fretting fatigue of Ti-6Al-4V under flat-on-flat contact", *Int. J. of Fatigue*, **21**, pp 663-669 (1999).
18. Kim, H.S. and Mall, S. "Investigation into three-dimentional effects of finite contact width on fretting fatigue", *Finite Element in Design and Analysis*, **41**, pp 1140-1159 (2005).

19. Dini, D. and Nowell, D. "Flat and rounded fretting contact problems incorporating elastic layers", *Int. J. of Mechanical Sciences*, **46**, pp 635-1657 (2004).

20. Dini, D. and Nowell, D. "Prediction of the slip zone friction coefficient in flat and rounded contact", *Wear*, **254**, pp 364-369 (2003).

21. Hills, D.A. and Nowell, D., *Mechanics of Fretting Fatigue*, Kluwer Academic Publishers (1994).

22. Erdogan, F. and Gupta, G.D. "On the numerical solution of singular integral equations", *Quarterly of Applied Mathematics*, pp 525-534 (1972).

23. Nowell, D. and Hills, D.A. "Mechanics of fretting fatigue", *Int. J. Mech. Sci.*, **29**(5), pp 355-365 (1987).

24. Muskhelishvili, N.I., *Singular Integral Equations*, Noordhoff Groningen (1953).

25. Hills, D.A., Nowell, D. and Sackfield, A., *Mechanics of Elastic Contacts*, Butterworth-Heinemann, Oxford (1993).

26. Tarafder, M., Tarafder, S., Ranganath, V.R. and Ghosh, R.N. "Finite element solutions for stress intensity factors in longitudinally cracked cylindrical components", *Int. J. Pres. Ves. & Piping*, **70**, pp 127-133 (1997).

27. McVeigh, P.A. and Farris, T.N., *American Institute of Aeronautics and Astronautics*, A99-24705 (1999).